Dynamics of GeoFlow
Thermal Convection in Rotating Spherical shells

B. Futterer

Dept. Aerodynamics and Fluid Mechanics,
Brandenburg University of Technology Cottbus, Germany

Topical Team
Geophysical Flow Simulation
Meeting 11/12 Dec 2008
BTU Cottbus

funded by: German Aerospace Center e.V. (DLR), grant number 50 WM 0122 & 50 WM 0822,
European Space Agency (ESA), grant number AO99-049, ESA Topical Team, grant number 18950/05/NL/VJ

Numerical and experimental visual data analysis

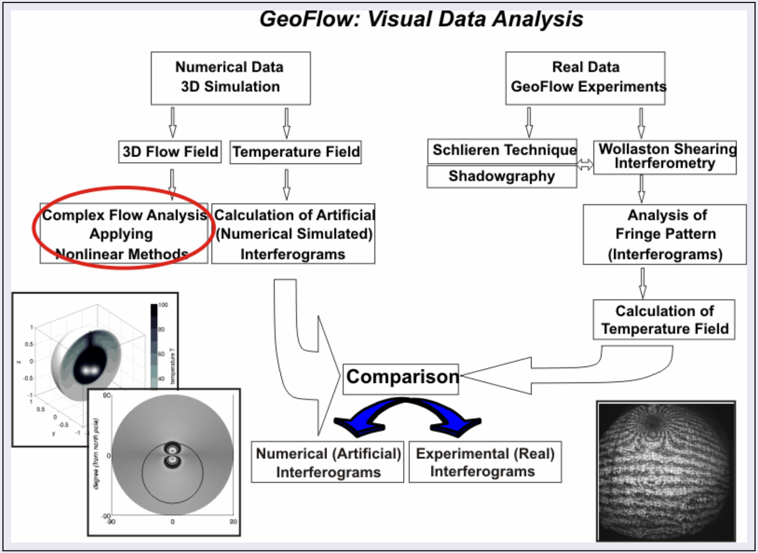

Outline

Boussinesq equations for convection in rotating spherical shells with dielectric force

$$\nabla \cdot \mathbf{U} = 0$$

$$Pr^{-1}\left[\frac{\partial \mathbf{U}}{\partial t} + (\mathbf{U}\cdot\nabla)\mathbf{U}\right] = -\nabla p + \nabla^2 \mathbf{U} + \frac{Ra_{central}\, T}{\beta^2 r^5}\,\hat{\mathbf{e}}_r - \sqrt{Ta}\,\hat{\mathbf{e}}_z \times \mathbf{U} + \widetilde{Ra}\; T\, r \sin\theta \hat{\mathbf{e}}_{eq}$$

$$\frac{\partial T}{\partial t} + \mathbf{U}\cdot\nabla T = \nabla^2 T$$

no-slip boundary conditions for velocity $\mathbf{U}$, temperature fixed $T(\eta) = 1$, $T(1) = 0$

Experimental constraints

				GeoFlow	outer core	mantle
gap width	$r_o - r_i [mm]$	13.5	$\rightarrow \eta$	0.5	0.37	0.55
viscosity	$\nu[m/s^2]$	$5 \cdot 10^{-6}$	$\rightarrow Pr$	64.64	0.1-1.0	∞, viscosity variable
high voltage temperature	$V_{rms}[V]$ $\Delta T[K]$	10 ≤ 10	$\}$ Ra	$\leq 1.4 \cdot 10^5$	$>10^{29}$	$10^6 - 10^8$
rotation rate	$n[Hz]$	≤ 2	$\rightarrow Ta$	$\leq 1.3 \cdot 10^7$	10^{30}	$<< 1$

Dynamics of GeoFlow in the experimental framework

- non-rotating case
  - coexisting of several modes (axisymmetric, cubic, m=5)
  - influence of initial conditions to reach different stable states
  - transition direct from steady to irregular flow with remnant tetrahedral symmetry
- rotating case
  - change of sign for drift velocity

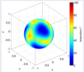
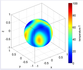

  - complex pattern drift

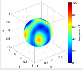
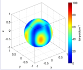

  - transition to stabilizing effects due to centrifugal forces
  - transition from steady via periodic to irregular flow

Stability diagram and flow states

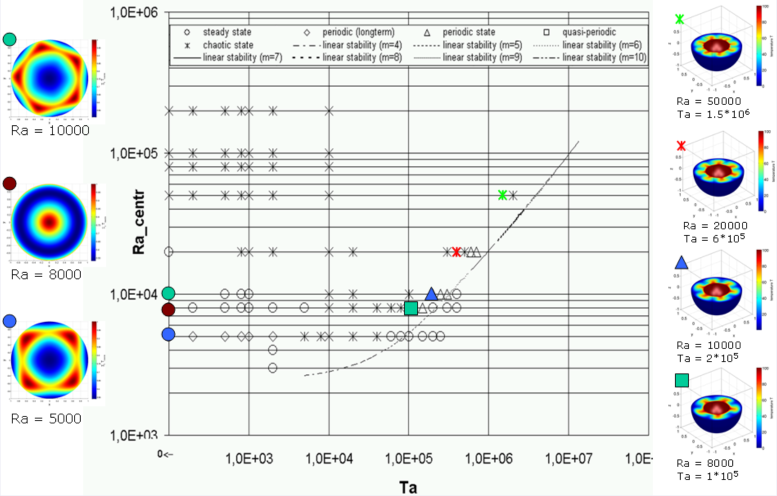

Focus for the rotating spherical shell

- onset of convection
  $\longrightarrow$ hysteresis in comparison to stability analysis
- pattern formation and drift analysis for low rotation
- pattern formation and drift analysis for medium and high rotation
  $\longrightarrow$ tangent cylinder
- transition to chaos (considered for Nusselt number of inner and outer sphere)
  $\longrightarrow$ steady / periodic / quasi-periodic / irregular

Stability diagram and flow states

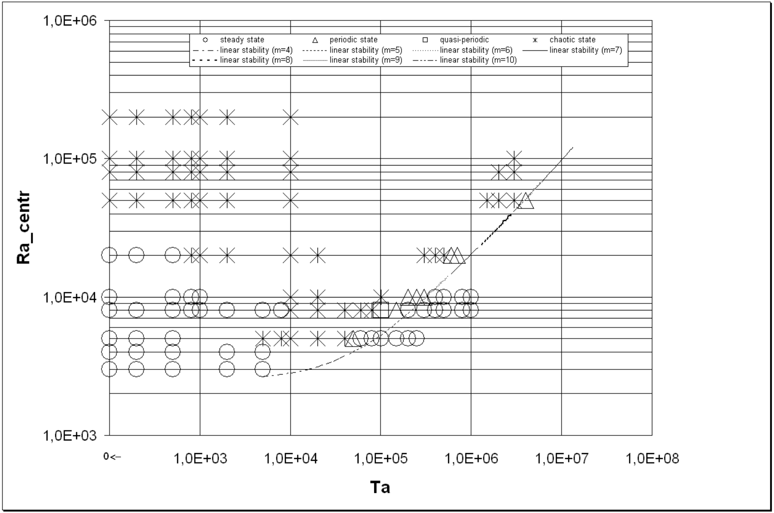

Ra_{centr} set, Ta increases: low rotation
temperature field visualized on spherical surface in the gap, scaled to 100 %

$Ra_{central}$	$Ta = 0$	$8 \cdot 10^2$	$2 \cdot 10^3$
$8 \cdot 10^3$	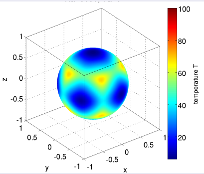 steady	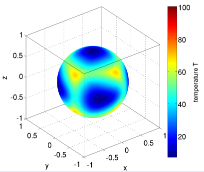 steady	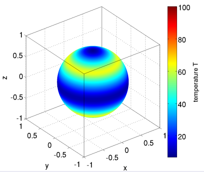 steady
$5 \cdot 10^3$	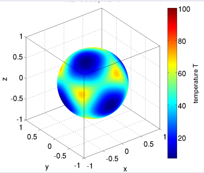 steady	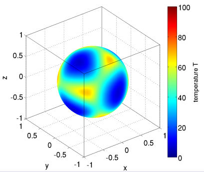 periodic longterm	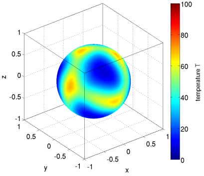 periodic longterm $n_{flow} = 0.000053\ Hz$ $n_{sphere} = 0.0244\ Hz$ drift prograd

Ra_{centr} set, Ta increases: intermediate rotation
temperature field visualized on spherical surface in the gap, scaled to 100 %

$Ra_{central}$ | $Ta = 1 \cdot 10^5$ | $1.5 \cdot 10^5$ | $2 \cdot 10^5$

$8 \cdot 10^3$

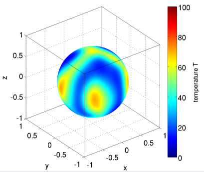

quasi-periodic
$n_{flow} = 250x0.0053\ Hz$
$n_{sphere} = 0.173\ Hz$
drift retrograd

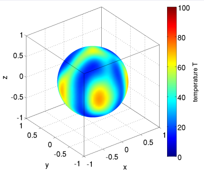

periodic
$n_{flow} = 0.0052\ Hz$
$n_{sphere} = 0.211\ Hz$
drift retrograd

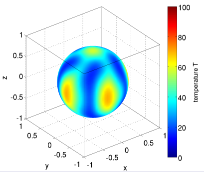

steady

$5 \cdot 10^3$

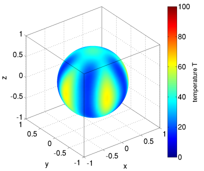

steady

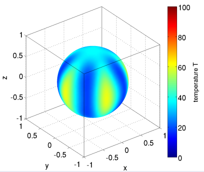

steady

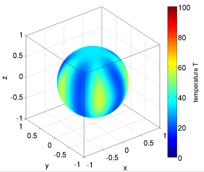

steady

GeoFlow experiment:
spherical Rayleigh-Bénard convection in self-gravitating force field

- radial gravity force by dielectrophoretic effect in microgravity environment
  - Yavorskaya et al. A simulation of central-symmetry convection in microgravity conditions. Acta Astronautica 11 (1984), 179–183
  - Hart et al. Space-laboratory experiments and numerical simulations of thermal convection in a rotating hemispherical shell with radial gravity. J. Fluid Mech. 173 (1986), 512–544
- spherical shell convection for non-rotating case
  - H.F. Busse & N. Riahi. Patterns of convection in spherical shells. Part 2. J. Fluid Mech. 123 (1982), 283–301
- convection in rotating spherical shells
  - A. Tilgner & F.H. Busse. Finite-amplitude convection in rotating spherical shells. J. Fluid Mech. 332 (1997), 359–376
  - C.A. Jones et al. The onset of thermal convection in a rapidly rotating sphere. J. Fluid Mech. 405 (2000), 157–179
  - F.H. Busse. Convective flows in rapidly rotating spheres and their dynamo action. Phys. Fluids 14 (2002), 1301–1313
  - R. Simitev & F.H. Busse. Prandtl-number dependence of convection-driven dynamos in rotating spherical shells. J. Fluid Mech. 532 (2005), 365–388

Aspects of GeoFlow experiment to be discussed

- force field dependence
  - Bifurcation analysis for influence of different force fields in geo-/astrophysical framework:
    P. Beltrame, V. Travnikov, M. Gellert, C. Egbers. GEOFLOW: Simulation of convection in a spherical gap under central force field . Nonlinear Processes in Geophysics, 13, 1-11
  - identification of Rossby waves in moderate rotation regime
    key words: dispersion relation
  - behaviour of columnar cells at tangent cylinder in rapid rotation regime
- Prandtl number dependence
  - pattern of convection (Rossby waves, columnar cells)
- steady states analysis by path following
- time dependency
  - transition from steady via periodic to irregular solutions
  - identification of irregularity

key words: Lyapunov exponent, EOF (empirisch orthogonale Funktion)

Coulomb force

- charged particle in electric field **E**
- $\mathbf{F}_\mathrm{C}(\mathbf{r}) = q\ \mathbf{E}$
- much stronger than dielectrophoretic force
- suppressed by using high-frequency AC voltage ($T_{el} \ll \tau$, τ – relaxation time of free particle)

Dielectrophoretic force

- due to polarisation of medium in electric fields (local dipoles)
- $\mathbf{F}_\mathrm{D}(\mathbf{r}) = \frac{1}{2}\mathbf{E}^2(\mathbf{r})\nabla\epsilon$
- acting as a ponderomotive force only in geometrically inhomogeneous field
- resulting movement only for dieletric inhomogenous media
- depends on gradient of **E**, not sign
- spherical geometry: $\mathbf{F}_\mathrm{D}(\mathbf{r}) \sim \mathbf{1/r^5}$
- acts as central force field (comparable to gravity)

GeoFlow constraints ...

- spherical shell system is geometrically inhomogenous
- experimental fluid is dielectric homogenous

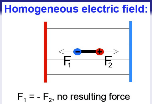

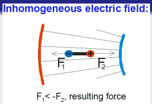

Setting up high voltage → acceleration due to dielectric force field

$$\mathbf{g_e} = \frac{1}{2\rho}\epsilon\epsilon_r \nabla|\mathbf{E}|^2 \quad \text{with} \quad \mathbf{E} = \frac{1}{r^2}\frac{r_i r_o}{r_o - r_i} V_0 \sin(\omega t)\hat{\mathbf{e}}_r$$

$$g_e = \frac{2\epsilon_0\epsilon_r}{\rho}\left(\frac{r_i r_o}{r_o - r_i}\right)^2 V_{rms}^2 \frac{1}{r^5}$$

ε_0 - dielectric constant, ε_r - relative permittivity, ρ - density, V_{rms} - voltage

GeoFlow specific values ...

$$\epsilon_0 = 8.854 \cdot 10^{-12}\ {}^{As}/_{Vm}, \quad \epsilon_r = 2.7,$$

$$\rho = 920\ {}^{kg}/_{m^3},$$

$$d = r_o - r_i = 27\ mm - 13.5\ mm = \ 13.5\ mm,$$

$$V_{rms} = 10\ kV$$

$$\rightarrow g_e|_{r_o} \approx 10^{-1} m/s^2 \qquad \text{compared to} \quad g \approx 10^1 m/s^2$$

→ microgravity conditions required!

Spectral method

- decomposition of primary variables into poloidal and toroidal parts
- decomposition of these into Chebyshev polynomials and spherical harmonics
- solving equations for spectral coefficients

$$e(r,\theta,\varphi,t) = \sum_{m=0}^{M} \sum_{\ell=m'}^{L} \sum_{k=1}^{K} e_{k\ell m} T_{k-1}(x) P_{\ell}^{|m|}(\cos\theta) e^{im\phi}$$

- truncation with (K,L,M)=(30,60,20) resp. (30,60,60) for non-rotating case
- R. Hollerbach. A spectral solution of the magneto-convection equations in spherical geometry. Int. J. Numer. Meth. Fluids 32 (2000), 773-797

Parameters

geometry	radius ratio	$\eta = \frac{r_i}{r_o}$
physical prop. of fluid	Prandtl number	$Pr = \frac{\nu}{\kappa}$
buoyancy (central force)	central Rayleigh number	$Ra_{central} = \frac{2\epsilon_0 \epsilon_r \gamma}{\rho \nu \kappa} \; V_{\mathrm{rms}}^2 \, \Delta T$
Coriolis force	Taylor number	$Ta = \left(\frac{2\Omega r_o^2}{\nu} \right)^2$
centrifugal force	additional Rayleigh number	$\widetilde{Ra} = \frac{\alpha \Delta T}{4} \; Ta \, Pr$

History of simulation work for GeoFlow

- Stability analysis for both cases $Ta = 0$ (determination of onset of convection) and $Ta \neq 0$ (influence of centrifugal force, modes of instabilities)
  - V. Travnikov, R. Hollerbach, C. Egbers. The GEOFLOW experiment on ISS. Part II: Numerical simulation. Adv. Space Res. 32 (2003), 181–189
  - V. Travnikov. Thermische Konvektion im Kugelspalt unter radialem Kraftfeld, Dissertation, Cuvillier Verlag Göttingen, 2004
- Bifurcation analysis (influence of different force fields in geo-/astrophysical framework)
  - P. Beltrame, V. Travnikov, M. Gellert, C. Egbers. GEOFLOW: Simulation of convection in a spherical gap under central force field . Nonlinear Processes in Geophysics, 13, 1-11
- Path following analysis (determination of stable and unstable solutions for stationary states for case $Ta = 0$)
  - K. Bergemann, L. Tuckerman, F. Feudel. GeoFlow: On symmetry-breaking bifurcations of heated spherical shell convection. J. Phys.: Conf. Ser. (in press)
- Direct numerical simulations (fluid flow and temperature field, calculation of interferograms)
  - M. Gellert, P. Beltrame, C. Egbers. The GeoFlow experiment - spherical Rayleigh-Bénard convection under the influence of an artificial central force field. J. Phys.: Conf. Ser. 14 (2005), 157-161
  - B. Futterer, M. Gellert, Th. von Larcher, C. Egbers. Thermal Convection in rotating spherical shells: An experimental and numerical approach within GeoFlow. Acta Astronautica 62 (2008), 300–307
  - B. Futterer, R. Hollerbach, C. Egbers. Geoflow: 3D numerical simulation of supercritical thermal convective states. J. Phys.: Conf. Ser. (in press)

Linear analysis for $Ta = 0$

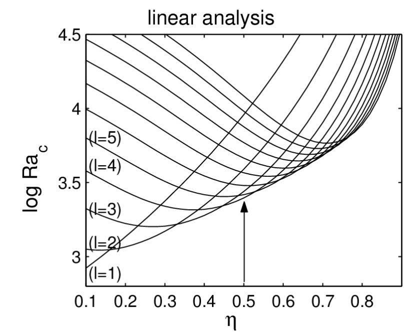

- critical Ra_{centr} for onset of convection independent on Pr
- larger $\eta \rightarrow$ larger critical mode l

Source: V. Travnikov, C. Egbers, R. Hollerbach. The GEOFLOW experiment on ISS. Part II: Numerical simulation. Adv. Space Res. 32 (2003), 181–189
V. Travnikov: Thermische Konvektion im Kugelspalt unter radialem Kraftfeld, Dissertation, Cuvillier Verlag Göttingen, 2004

Linear analysis for $Ta \neq 0$

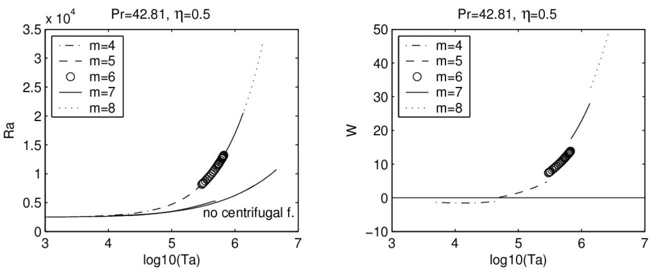

- shape of stability curves nearly independent on *Pr*
- instability due to Hopf bifurcation
- for large *Ta*: $Ra_{centr} \sim Ta^{2/3}$
  [P.H. Roberts. On the thermal instability of a rotating-fluid sphere containing heat sources. Philos. Trans. R. Soc. London 263 (1968), 93-117]
- drift velocity W changes sign (slows down or fastens rotation)

Source: Travnikov et al. (2003), Travnikov (2004)

Path-following analysis for stationary solutions at $Ta = 0$

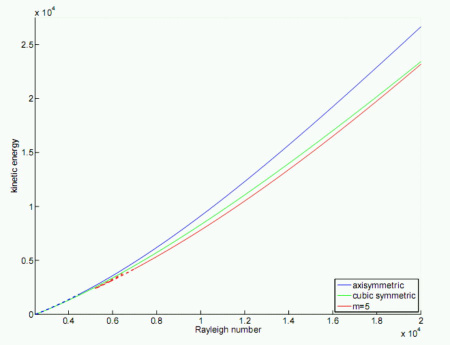

- existence of multistability (axisymmetry, cubic, $m = 5$)
- sudden onset of chaos at $Ra > 28000$
- hysteresis behaviour of the chaotic branch resulting in frozen states with tetrahedral symmetry

Source: K. Bergemann, L. Tuckerman, F. Feudel. GeoFlow: On symmetry-breaking bifurcations of heated spherical shell convection. J. Phys.: Conf. Ser. (in press)
K. Bergemann: Konvektion im Kugelspalt: Numerische Untersuchung und Bifurkationsanalyse am Beispiel des GeoFlow-Experimentes, Diplomarbeit, Universität Potsdam, 2008

Timeseries of kinetic energy

irregular

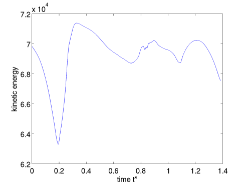

quasiperiodic

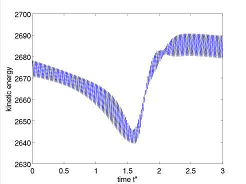

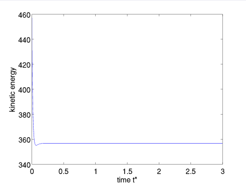

steady

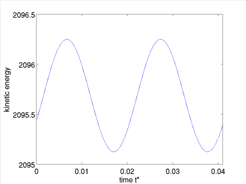

periodic